Densely packed Gd(III)-chelates with fast water exchange on a calix[4]arene scaffold: a potential MRI contrast agent

Daniel T. Schühle,[a,b] Miloslav Polášek,[c] Ivan Lukeš,[c] Thomas Chauvin,[d] Éva Tóth,[d] Jürgen Schatz,[b,e] Ulf Hanefeld,[a] Marc C. A. Stuart[f] and Joop A. Peters*[a]

A pyridine-N-oxide functionalized DOTA analogue has been conjugated to a calix[4]arene and the corresponding Gd-complex was characterized with respect to its suitability as MRI contrast agent. The compound forms spherical micelles in water with a *cmc* of 35 μM and a radius of 8.2 nm. The relaxivity of these aggregates is 31.2 s^{-1} mM^{-1} at 25 °C and 20 MHz, which corresponds to a molecular relaxivity of 125 s^{-1} mM^{-1}. The high relaxivity mainly originates from the short τ_M (72.7 ns) and the size of the micelles. The interaction with bovine serum albumin (BSA) was studied and an observed relaxivity of up to 40.8 s^{-1} mM^{-1} (163.2 s^{-1} mM^{-1} per binding place) at 20 MHz and 37 °C was found in the presence of 2.0 mM protein.

Introduction

Magnetic resonance imaging (MRI) is one of the most powerful techniques in medical diagnostics. Usually, the water ^1H-signal is detected and the contrast is generated by differences in proton density and longitudinal (T_1) or transverse (T_2) relaxation time. To enhance the contrast in T_1-weighted images, mainly gadolinium(III) based contrast agents (CAs) are administered prior to the examination.[1–6] To avoid the release of the toxic free lanthanide ion, strong chelators such as 1,4,7,10-tetracarboxymethyl-1,4,7,10-tetraazacyclododecane (DOTA) and derivatives thereof are used. The contrast that can be achieved with a certain amount of CA depends on the choice of the ligand because that determines its physico-chemical properties and its distribution in the patient.

Good performance of the contrast agent per mmol Gd is desirable, *i.e.* the millimolar longitudinal proton relaxivity (r_1) of the contrast agent has to be as high as possible. The two commonly used ways to optimize relaxivity are to increase the rotational correlation time (τ_R) of the CA and to optimize the residence time of a water molecule directly bound to the metal center (τ_M) to 20–40 ns (at 60 MHz and 25 °C).

Recently, we have shown that calix[4]arenes are versatile building blocks in the design of MRI CAs.[7–10] They allow the introduction of four chelating groups on the *upper rim*, enable

further functionalization at the *lower rim*, and they turned out to be very rigid, which has a beneficial effect on the value of τ_R, and thus the relaxivity.[7] The rigidity is mainly due to the densely arranged chelators on the calixarene that leads to hindered rotation within the molecule. The previously studied **1** (see Fig. 1) showed micelle formation and interaction with human serum albumin (HSA). Both effects result in a significant increase of the molecular volume, which is reflected in a longer τ_R and, therefore, in a higher relaxivity.

The relaxivity of **1** is limited mainly by its long τ_M.[7] Therefore, we now decided to replace the DOTA moieties in **1** by chelator **2** (Fig. 1). The Gd(III) complex of the parent **2** has a τ_M of 34 ns at 25 °C and therefore, is optimal in this respect.[11–13] The rigid pyridine moiety, the presence of the carboxylic acid group attached to the pyridine ring and the possibility to convert this group into an amide with partial double bond character makes **2** a good ligand for conjugation to other molecules. First attempts to increase the relaxivity of systems based on **2** by increasing τ_R were to couple it to PAMAM-dendrimers.[14] The unexpectedly small increase in relaxivity of those conjugates was attributed to local motions in the rather flexible dendrimer core that reduce the effective rotational correlation time.

In this paper, we describe the synthesis of **3** along with the evaluation of its relaxometric properties.

Results and discussion

Synthesis

Conjugate **3** was obtained from starting materials described before.[13,15] As previously observed during the synthesis of compound **1**, the crucial step is the amide bond formation of tetraaminocalix[4]arene **4** and the carboxy functionalised chelator (Scheme 1).[7]

The reaction was performed using six equivalents of **5** as its Hünig's base (DIPEA) salt and O-(benzotriazol-1-yl)-N,N,N′,N′-tetramethyluronium tetrafluoroborate (TBTU) at room temperature. After three days the conversion was complete as monitored by

[a]*Biocatalysis and Organic Chemistry, Department of Biotechnology, Delft University of Technology, Julianalaan 136, 2628, BL Delft, The Netherlands. E-mail: j.a.peters@tudelft.nl; Fax: +31(0)152781415; Tel: +31(0)152785892*
[b]*Institute of Organic Chemistry I, University of Ulm, Albert-Einstein Allee 11, 89081, Ulm, Germany*
[c]*Department of Inorganic Chemistry, Charles University, Hlavova 2030, 12840, Prague 2, Czech Republic*
[d]*Centre de Biophysique Moléculaire, CNRS, Rue Charles Sadron, 45071, Orléans, France*
[e]*Department of Chemistry and Pharmacy, University of Erlangen-Nürnberg, Henkestraße 42, 91054, Erlangen, Germany*
[f]*Groningen Biomolecular Sciences and Biotechnology Institute, Electron Microscopy Group, University of Groningen, Nijenborgh 4, 9747, AG Groningen, The Netherlands*
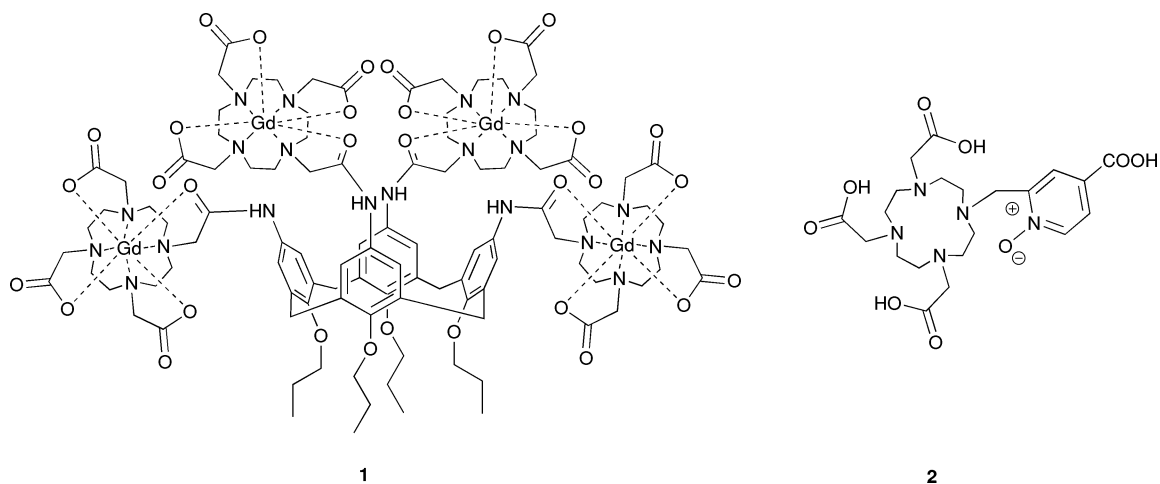
Fig. 1 Structures of calixarene **1** and DO3A-py^{NO-C} **2**.

HPLC. The reaction mixture contained only **6** and low molecular weight compounds that were removed by ultrafiltration. The mixture was dissolved in a methanolic NH$_4$OAc buffer to break ion pairs between the chelator and hydroxybenzotriazole (HOBt) and subjected to continuous ultrafiltration first with this buffer and then with pure methanol. A smooth deprotection of the tBu-ester groups by TFA and subsequent complexation of the unpurified intermediate dodecaacid with an excess of GdCl$_3$·6H$_2$O gave **3**, which was purified by ultrafiltration after complexation of the excess of Gd(III) with EDTA.

Aggregation

Previously, we have shown that above the critical micelle concentration (*cmc*) of 0.21 mM, calix[4]arene **1** forms micelles with a radius of 2.2 nm in aqueous solution.[7] Dynamic light scattering (DLS) on a 3.7 mM sample of **3** at 25 °C (see Fig. 2) illustrates that this compound also self-aggregates. The presence of two peaks in the DLS spectra shows that there are two different

Scheme 1 Preparation of **3**: (i) TBTU, MeCN, 3 d, rt; (ii) TFA/DCM 50 : 50, overnight, rt; (iii) GdCl$_3$·6H$_2$O, NaOH, H$_2$O, pH 7, 1 d, rt.
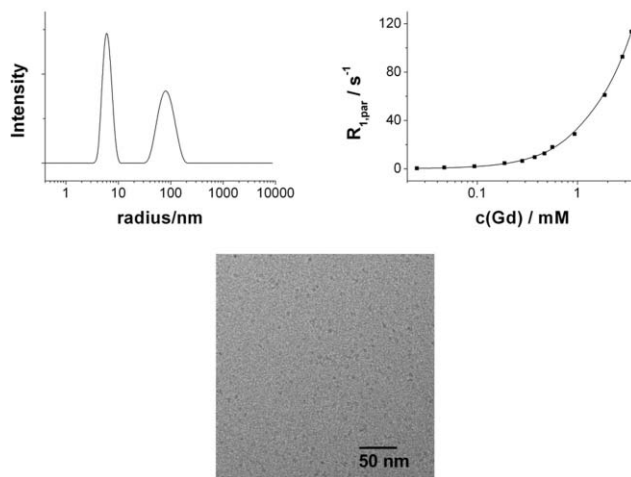
Fig. 2 DLS (3.7 mM, 25 °C) (top left), relaxometric ^{1}H NMR measurements (25 °C, 20 MHz) (top right) as well as cryo-TEM (down) of **3**. The line indicates the result form the fitting of the experimental data with eqn (1) and 2.

aggregates present with hydrodynamic radii of 8.2 and 85.0 nm. An increase of temperature to 50 °C did not result in significant changes indicating that these aggregates are very stable. It needs to be stressed that the intensity weighted DLS spectra depicted in Fig. 2 do not reflect the quantitative composition of the solution. Particles that are a factor of 10 larger than others scatter light approximately one million times more than the smaller aggregates.[16] This means that **3** is almost exclusively present as small, 8.2 nm micelles with only traces of larger aggregates. The narrow size distribution for the small aggregates is an indication that they are spherical micelles. This shape was confirmed by cryo-TEM (Fig. 2). There is no evidence of larger aggregates in the cryo-TEM, which is another indication that the concentration of these larger aggregates is negligible.

The *cmc* of the micelles was determined with the use of relaxometric NMR measurements.[17] This method makes use of the increase in relaxivity of Gd-complexes upon aggregation due to increase of τ_R. Therefore, the paramagnetic relaxation rate (R_1) was measured as a function of the concentration of Gd (c_{Gd}) in **3**. In the absence of self aggregation, a plot of R_1 versus c_{Gd} should be a straight line. If there is self aggregation, R_1 is a sum of two linear relations, starting at the *cmc*.

$$\frac{1}{T_1} = \frac{1}{T_{1,obs}} - \frac{1}{T_{1,dia}} = R_1 = 4cmc \cdot r_1^{n.a.} + (c_{Gd} - 4cmc) \cdot r_1^{a} \tag{1}$$

$$R_1 = c_{Gd} r_1^{n.a.} \tag{2}$$

Above the *cmc*, eqn (1) describes R_1 as a function of the concentration of Gd (c_{Gd}), the relaxivity of the monomer ($r_1^{n.a.}$) and the aggregates (r_1^{a}) as well as the *cmc*. Eqn (2) describes R_1 as a function of c_{Gd} below the *cmc*.

The value of $r_1^{n.a.}$ was determined to be 17.1 s⁻¹ mM⁻¹ using an independent measurement of the relaxivity of a sample well below the *cmc* (6.25 μM). The data from the relaxometric measurements as a function of c_{Gd} at 25 °C (Fig. 2), were fitted using eqn (1) and 2 keeping $r_1^{n.a.}$ fixed to 17.1 s⁻¹ mM⁻¹. The best-fit value for the *cmc* is 35 ± 5 μM and that for r_1^{a} 33.5 ± 0.5 s⁻¹ mM⁻¹ at 25 °C and 20 MHz. It should be noted that only one *cmc* was observed, which once again indicates that the larger aggregates detected in the DLS are present in negligible amounts.

At 37 °C, a strictly linear dependence of R_1 on the concentration was found for values of c_{Gd} between 0.025 mM and 3.70 mM. This indicates that the *cmc* is even smaller at higher temperatures, which is typical for noncharged surfactants.

The lower *cmc* of **3** compared to **1** as well as the presence of a very small fraction of an additional type of larger aggregates suggests that stronger hydrophobic interactions exist among the chelates **3**. This can be attributed to the relatively large hydrophobic part in this compound due to the presence of the pyridine-*N*-oxide moieties. In addition, this may give rise to a different shape of the monomer and thus to different geometries of the aggregates.

Water exchange

The most suitable technique to assess the water exchange kinetics is variable temperature ¹⁷O NMR. From chemical shifts (ω), longitudinal (T_1) and transverse (T_2) relaxation times of the water ¹⁷O resonance, the reduced parameters ($\Delta\omega_r$, T_{1r}, T_{2r}) can be calculated by using the mole fraction of the Gd-bound water (P_m)

Table 1 Parameters obtained from simultaneous fitting of the variable temperature ¹⁷O NMR data of a 22.9 mM sample of **3**

Parameter	Best-fit value
$\Delta H^{\neq}$ [kJ mol⁻¹]	38.4 ± 2.8
τ_M^{298} [ns]	72.7 ± 9.9
τ_R^{298} [ps]	754 ± 20
E_R [kJ mol⁻¹]	9.64 ± 0.72
Δ^2 [10²⁰ s⁻¹]	0.46 ± 0.04
τ_v^{298} [ps]	2.70 ± 0.20
A/ħ [10⁶ rad s⁻¹]	−3.32 ± 0.13

and the corresponding parameters of a reference sample ($\Delta\omega_A$, T_{1A}, T_{2A}).[19]

$$\Delta\omega_r = \frac{1}{P_m}(\omega - \omega_A) \tag{3}$$

$$\frac{1}{T_{1r}} = \frac{1}{P_m}\left[\frac{1}{T_1} - \frac{1}{T_{1A}}\right] \tag{4}$$

$$\frac{1}{T_{2r}} = \frac{1}{P_m}\left[\frac{1}{T_2} - \frac{1}{T_{2A}}\right] \tag{5}$$

The measurements were performed at 7.05 T and at relatively high concentration (91.7 mM Gd corresponding to 22.9 mM **3**). At this high concentration, the contribution of monomeric **3** can be neglected and the data are representative for micellar **3**.

The almost constant value found for $\Delta\omega_r$ and the fact that T_{2r} has no maximum in the studied temperature range means that **3** is in the fast exchange regime for all temperatures. The best fit-values obtained from a fitting of the experimental data with the appropriate equations of the temperature dependence of these reduced parameters are compiled in Table 1.[18] The curves in Fig. 3 are calculated with these values.

The parameters describing the water exchange kinetics, τ_M and its activation enthalpy $\Delta H^{\neq}$ are in the expected range for conjugates with **2**.[11] The slightly longer τ_M found for **3** can be attributed to the fact that the conversion of the carboxylic acid to an amide has an effect on the electron density in the aromatic ring and therefore also on the oxygen atom coordinated to the metal center. Similar effects were observed for PAMAM conjugates with **2**.[14]

The best-fit values for the rotational dynamics are in the expected range for aggregates of this type and the electronic parameters, namely the mean square zero-field splitting energy (Δ^2) and its rotational correlation time (τ_v^{298}), are almost identical to those found for the parent system **2**.[11,12]

Relaxivity

Nuclear magnetic relaxation dispersion (NMRD) is a widely used technique in MRI research. The relaxivity r_1 as a function of the magnetic field (B) or the proton Larmor frequency ($\upsilon(^1H)$) is called NMRD profile. From these profiles, important parameters such as mainly the electronic parameters as well as τ_R can be obtained by fitting them with the appropriate equations.[18]

Owing to the very low *cmc* of **3**, it was not possible to measure NMRD profiles of monomeric **3**. An NMRD profile of micellar **3** was acquired at 925 μM concentration (Fig. 4). It shows a peak around 20 to 40 MHz which is typical for large, slowly tumbling systems. The relaxivity of **3** (31.2 s⁻¹ mM⁻¹ per Gd³⁺
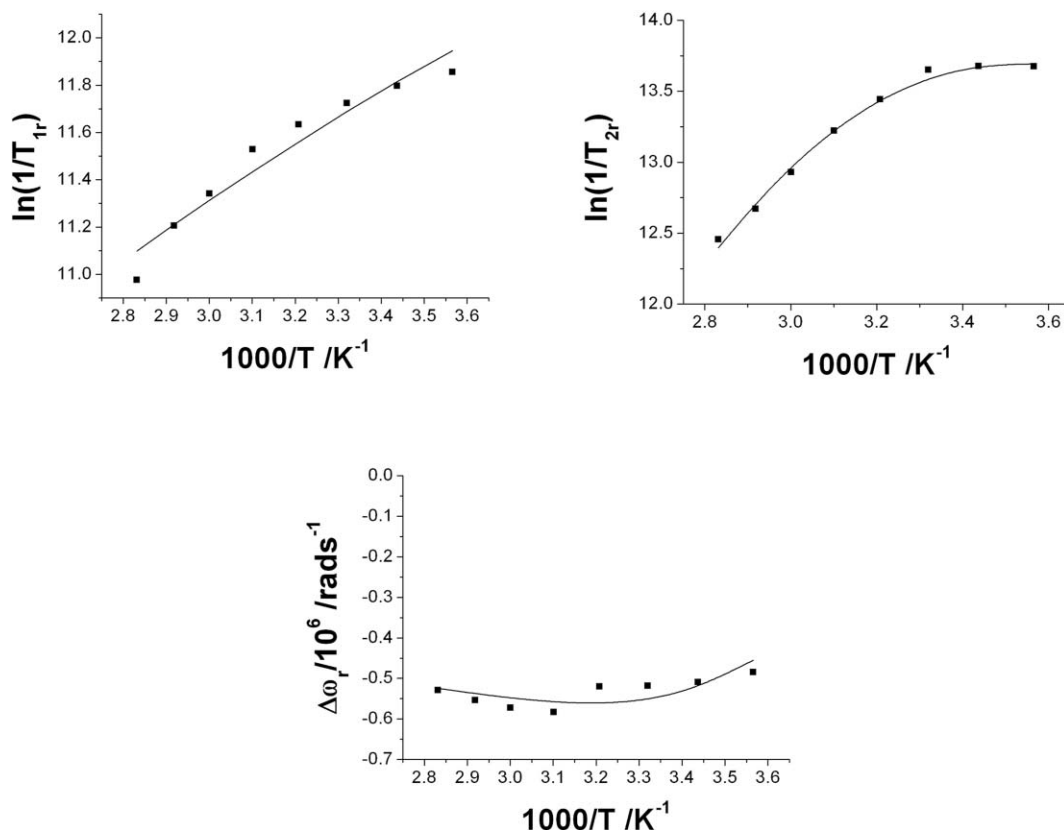
Fig. 3 Temperature dependence of reduced longitudinal (T_{1r}) and transverse (T_{2r}) relaxation times and angular frequency ($\Delta\omega_r$) of a 22.9 mM aqueous solution of **3** at 7.05 T (curves represent results from the fittings, see Experimental).
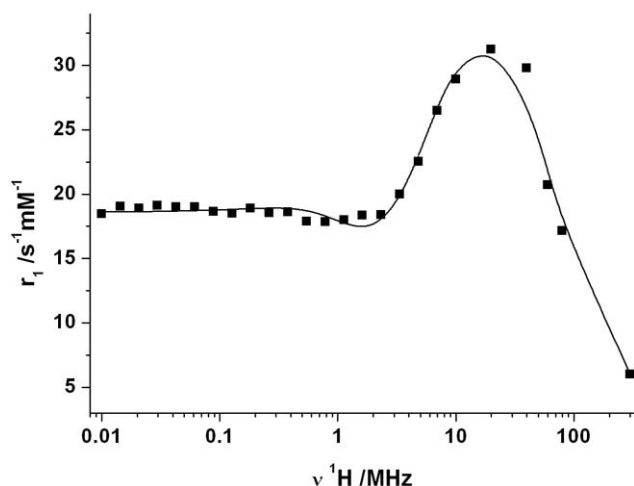
Fig. 4 NMRD profile of a 925 µM solution of **3** at 25 °C. The curve indicates the result from the fitting.

and 125 s⁻¹ mM⁻¹ per molecule at 25 °C and 20 MHz) is about twice of that of conjugates with generation 4 PAMAM dendrimers (16 s⁻¹ mmol⁻¹ for G4-Gd-**2**) and is even more superior to the generation 1 analogue (G1-Gd-**2**).[14] This can only be caused by either a higher τ_R due to aggregation or higher internal rigidity.

To gain more insight into the reasons for the enhanced relaxivity of micellar **3** compared to its PAMAM analogues, the NMRD

profile was analysed with the Solomon-Bloembergen-Morgan theory for the inner sphere contribution, extended by the Lipari-Szabo approach, and the Freed equations for the outer sphere contribution.[18,19] In the Lipari-Szabo approach, τ_R of slowly tumbling molecules is described by two different and independent tumbling times that contribute to the overall motion: a fast local (τ_l) and a slower global (τ_g) correlation time.[1] The extent to which they contribute to τ_R is expressed by an order parameter S^2 with $S^2 = 1$ for a perfectly rigid system (τ_l is negligible) and $S^2 = 0$ for flexible compounds where internal motions fully dominate the rotational dynamics. To limit the number of parameters involved in the fitting, the parameters that describe the water exchange kinetics were fixed to the values found by ¹⁷O NMR (Table 1). A simultaneous fit of the ¹⁷O and NMRD data was not possible which might be ascribed to different aggregation behaviours at the different concentrations needed for the measurements. A good fit for the NMRD profile was obtained for the values listed in Table 2. For comparison, previously published data for **1** and for PAMAM conjugates of **2** are included in Table 2.

In comparison to micellar **1**, not only τ_M is much more favourable, but also the overall rotational dynamics is improved. This is due to the larger radius of the spherical micelles formed by **3** (8.2 nm compared to 2.2 nm for **1**). The rather small value for τ_l indicates a fast internal motion within the micelles and therefore, a loss in rigidity compared to **1**. The order parameter S^2 shows that the contribution of internal motion to the overall rotational dynamics is significant and that the rotations of the

Table 2 Relaxometric parameters for selected Gd(III) chelates (italic values were fixed during the fitting processes)

	1[a]	Gd-2[b]	G1-Gd-2[c]	G4-Gd-2[c]	3
τ_M^{298} [ns]	1200 ± 120[d]	34 ± 0.1	55[d]	55 ± 2	72.7[d]
τ_R^{298} [ps]	1802 ± 110[e]	93 ± 13	$\tau_g = 570 \pm 30$ $\tau_l = 124 \pm 8$	$\tau_g = 1040 \pm 100$ $\tau_l = 138 \pm 4$	$\tau_g = 2621 \pm 196$[e] $\tau_l = 163 \pm 52$[e]
S^2	—	—	0.35 ± 0.03	0.38 ± 0.03	0.44 ± 0.03[e]
Δ^2 [10^{20} s^{-1}]	0.051 ± 0.006[e]	0.90 ± 0.11	0.105 ± 0.006	0.083 ± 0.002	0.042 ± 0.003[e]
τ_v^{298} [ps]	61.9 ± 2.2[e]	4.7 ± 0.6	49 ± 2	56 ± 1	95 ± 4[e]
r_1 [s^{-1} mM^{-1}][f]	18.3[g]	5.7	11.0	15.6	31.2
Density of Relaxivity [(g l^{-1})$^{-1}$s^{-1}][f]	26.0[g]	8.7	13.5	17.7	39.2

[a] values adapted from Ref. 7. [b] see Ref. 11; values obtained by a simultaneous fit of ^{17}O and NMRD data. [c] see Ref. 14; values obtained by a simultaneous fit of ^{17}O and NMRD data. [d] values obtained by a fit of ^{17}O data. [e] values obtained by a fit of NMRD data of the micellar compound at 25 °C. [f] at 25 °C and 20 MHz. [g] at 37 °C and 20 MHz.

chelates around the connection point to the calixarene are not hindered effectively. The larger distance between the metal ion and the platform leads to more flexibility due to rotations and/or vibrations.

This can be rationalized by the additional bonds between the metal and the calixarene core that increase the distance between the bulky chelates and therefore, decrease the steric repulsions between them. The electronic parameters follow the trend observed for Gd-2 and the PAMAM conjugates. For G4-Gd-2, we assume a similar radius as found for other PAMAM dendrimers conjugated with DOTA based chelators of about 6 nm, whereas the generation 1 analogue measures around 2 nm.[20] Micellar 3 measures 8.2 nm, which makes it the largest particle studied up to now for conjugates with 2. Upon an increase of size, generally Δ^2 decreases whereas τ_v increases.[21]

The order parameter S^2 for the micellar 3 is in the same range as that found for the PAMAM conjugates of 2.[14] This means that the internal motions in 3 and the dendrimers contribute to about the same extent to the overall rotational dynamics and that there is no rigidification within 3. To confirm that τ_g is the main factor causing the two fold enhanced relaxivity of the micellar 3 with respect to that for the generation 4 dendrimer, a simulation was performed. All parameters for 3 were kept at the values mentioned in Table 2 with the exception of τ_g, which was changed to the value found for G4-Gd-2. The simulated relaxivity at 20 MHz and 25 °C is 18.2 s^{-1} mmol^{-1}, which is very close to the value observed for G4-Gd-2 (15.6 s^{-1} mmol^{-1}) confirming that the increase of relaxivity for micellar 3 is indeed due to its larger size.

For molecular imaging applications, the molar relaxivity, r_1 is not always the most appropriate parameter to express the efficiency of a CA. It is often more important to know the payload of Gd that can be delivered per mass unit of CA. Therefore, the density of relaxivity was introduced, which is defined as the relaxation rate enhancement by a unity mass of the CA.[22] It is calculated by dividing the relaxivity per particle by its molecular weight. Micellar 3 has a density of relaxivity of 39.2 (g l^{-1})$^{-1}$ s^{-1} at 20 MHz and 25 °C. This is very close to that of the benchmark metallostar (43.3 (g l^{-1})$^{-1}$ s^{-1}) which has one of the highest densities of relaxivity reported so far.[22] The high density of relaxivity of 3 can be attributed to both optimized τ_M and rotational motions that even compensate the fact that the metallostar has two inner sphere water molecules.

Interaction with BSA

As shown in previous studies on lanthanide binding calixarenes, this class of compounds is able to interact with albumins.[7,23,24] Therefore, binding studies with 3 and bovine serum albumin (BSA) were performed.[23] The increase of τ_R upon binding of 3 to albumin leads to an increase in r_1. A sample of 3 with a concentration well below the *cmc* (6.25 μM) was titrated with BSA at 37 °C and 20 MHz. The peptide concentration (c_{BSA}) was varied between 0.1 and 2.0 mM (Fig. 5). The relaxivity shows a stepwise increase in relaxivity upon an increase of the BSA concentration. A sample with a four times higher concentration of 3 showed a similar behaviour (data not shown). In both cases, no plateau in the relaxivity was reached indicating that the binding is rather weak, as was also observed for 1.[7] The stepwise increase of r_1 upon an increase of the protein concentration might be rationalized by binding of 3 to different binding sites in BSA, probably on the surface of the protein.
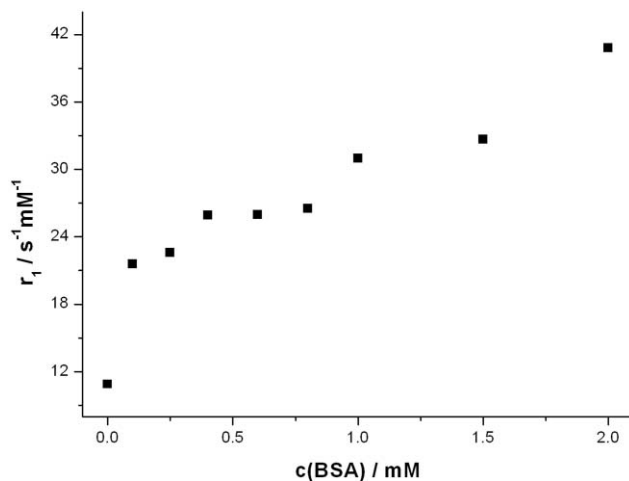
Fig. 5 Relaxometric BSA titration of a 6.25 μM solution of 3 (37 °C, 20 MHz).

Due to the weak binding, it was not possible to determine accurate binding constants of 3 to BSA. For practical applications, the observed relaxivity ($r_{1,obs}$) of the solution, which is defined as the relaxivity of 3 in the presence of the albumin after correction for the diamagnetic contribution of the protein is of much greater

relevance.[25] For many albumin targeted CAs, r_1 is rather high but due to relatively weak binding, $r_{1,obs}$ is in the range of 16 to 28 s^{-1} mM^{-1} for solutions containing the physiological albumin concentration (0.67 mM).[25] As shown in Fig. 5, between 0.6 mM and 0.8 mM BSA concentration, the relaxivity of a 6.25 μM solution of **3** under these conditions has an $r_{1,obs}$ of around 26 s^{-1} mM^{-1}, per gadolinium, which corresponds to a relaxivity of 104 s^{-1} mM^{-1} per mM **3** and per BSA binding site. The observed relaxivity could be further enhanced by shifting the equilibrium to the BSA-bound form. This is demonstrated by the fact that at high c_{BSA}, a relaxivity of 40.8 s^{-1} mM^{-1} (per mM **3** 163.2 s^{-1} mM^{-1}) was observed.

To obtain more information about the relaxivity of **3** in the presence of albumin, an NMRD measurement of **3** was performed in the presence of 0.6 mM BSA (Fig. 6). The rather narrow peak at around 20 MHz is a strong indication for the formation of slowly tumbling BSA adducts. Therefore, **3** has potential as an MRI contrast agent for application in angiography.
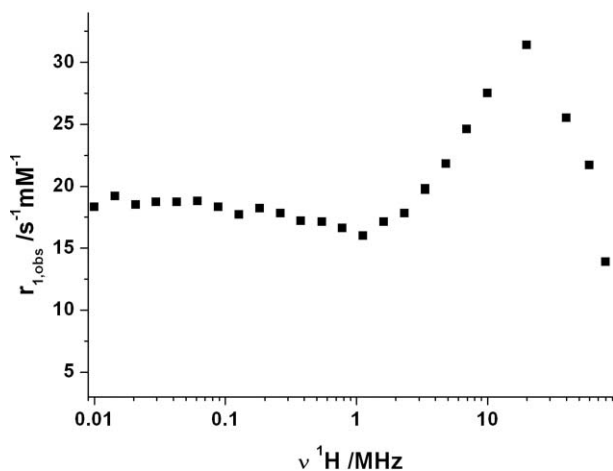
Fig. 6 NMRD profile of a 6.25 μM solution of **3** in the presence of 0.6 mM BSA at 37 °C.

Conclusion

The compound presented in this study is a promising candidate for MRI applications. Its self-aggregation in water results in spherical micelles that appear already at low concentration (<25 μM at 37 °C). Thanks to an almost optimal value of τ_M, **3** exhibits good relaxivities both in monomeric and aggregated form as well as in the presence of BSA. The high relaxivities of the supramolecular species are due to their large sizes and not to an intramolecular rigidification. With this compound, a relaxivity of more than 163 s^{-1} mM^{-1} per calixarene molecule could be achieved. The density of relaxivity at 20 MHz and 25 °C of this compound is extremely high (39.2 (g l^{-1})$^{-1}$ s^{-1}), which opens up possibilities to use similar compounds in the molecular imaging of, for example, receptors on cell surfaces.

Experimental

General considerations

Compounds **2** and **4** were readily available following literature procedures.[15] All other chemicals were of commercial grade

and used without further purification. The NMR spectra were acquired on a Varian Inova-300 spectrometer.

Preparation of 5,11,17,23-tetrakis-(*tert*-butyl-DO3A-py$^{NO–C}$-acetamidyl)-25,26,27,28-tetrapropoxy-calix[4]arene (6). In an inert atmosphere, the DIPEA salt of *tert*-butyl-DO3A-py$^{NO–C}$-carboxylic acid (**5**) (292 mg, 367 μmol) and TBTU (162 mg, 367 μmol) were stirred in anhydrous MeCN (8 ml) for 1 h. This was then added to a solution of 5,11,17,23-tetraamino-25,26,27,28-tetrapropoxy-calix[4]arene (**4**) (40 mg, 61.3 μmol) in anhydrous MeCN (20 ml). After stirring the mixture for 3 d at ambient temperature, the solvent was removed and the product was purified by ultrafiltration over a 1 kDa membrane using continuous elution with a 0.05 M NH$_4$OAc solution in MeOH followed by pure methanol. After evaporation of the solvent, the product was obtained as a fluffy slightly yellow powder by lyophilisation from benzene (176 mg, 54.4 μmol, 89%).

^{1}H NMR (300 MHz, MeOD-d$_4$, 55 °C, TMS): δ = 1.06 (12 H, t, J = 7.4 Hz, C*H*$_3$), 1.40, 1.46 (72 and 36 H, 2 s, *tert*-Bu), 2.01 (8 H, sext, J = 7.4 Hz, C*H*$_2$-CH$_3$), 2.81–3.02 (64 H, m, N–C*H*$_2$-C*H*$_2$), 3.26 (4 H, d, J = 13.2 Hz, ArC*H*$_2$Ar), 3.36, 3.43 (32 H, 2 br s, N–C*H*$_2$-CO), 3.96 (8 H, t, J = 7.4 Hz, OC*H*$_2$CH$_2$), 4.60 (4 H, d, J = 13.2 Hz, ArC*H*$_2$Ar), 7.18 (8 H, s, Ar-*H*), 7.80 (4 H, br m, Ar-*H*), 8.30 (4H, d, J = 6.9 Hz, Ar-*H*), 8.34 (4H, br s, Ar-*H*). ^{13}C NMR (75 MHz, MeOD-d$_4$, 55 °C, TMS): δ = 9.63 (*C*H$_2$CH$_3$), 23.24 (*C*H$_2$CH$_3$), 27.34 (OC(*C*H$_3$)$_3$), 31.13 (Ar*C*H$_2$Ar), 46.27, 50.39, 50.90, 53.75 (N*C*H$_2$*C*H$_2$N, N*C*H$_2$COO), 77.09 (O*C*H$_2$CH$_2$), 81.37, 81.48 (O*C*(CH$_3$)$_3$), 118.58, 121.05, 121.59, 132.24, 135.20, 143.79, 148.94, 154.00, 160.35 (Ar-*C*), 171.40, 171.53 (*C*OtBu), 178.99 (*C*ONH). ESI-MS: calc.: m/z = 1660.08 (M+2 K)$^{2+}$, found: 1659.97.

Preparation of 5,11,17,23-tetrakis-(DO3A-py$^{NO–C}$-acetamidyl) 25,26,27,28-tetrapropoxy-calix[4]arene. 5,11,17,23-Tetrakis-(*tert*-butyl-DO3A-py$^{NO–C}$-acetamidyl)-25,26,27,28-tetrapropoxy-calix[4]arene (**6**) (99.0 mg, 30.5 μmol) was dissolved in a mixture of TFA/DCM 50 : 50 (6 ml). After stirring overnight, the solvents were evaporated and the product was lyophilized from water to give the title compound (113.8 mg) as its TFA salt. The compound was not purified since the TFA as well as inorganic impurities can easily be removed after complexation by ultrafiltration.

^{1}H NMR (300 MHz, D$_2$O, 90 °C): δ = 1.57 (12 H, t, J = 7.0 Hz, C*H*$_3$), 2.47 (8 H, sext, J = 7.0 Hz, C*H*$_2$-CH$_3$), 3.81–4.99 (112 H, m, N–C*H*$_2$-C*H*$_2$, ArC*H*$_2$Ar, N–C*H*$_2$-CO, OC*H*$_2$CH$_2$), 7.68 (8 H, s, Ar-*H*), 8.37 (4 H, d, J = 6.3 Hz, Ar-*H*), 8.62 (4H, s, Ar-*H*), 8.87 (4H, d, J = 6.3 Hz, Ar-*H*). ^{13}C NMR (75 MHz, D$_2$O, 90 °C): δ = 10.9 (*C*H$_2$CH$_3$), 23.86 (*C*H$_2$CH$_3$), 31.70 (Ar*C*H$_2$Ar), 50.91, 51.12, 53.52, 55.04, 55.70 (N*C*H$_2$*C*H$_2$N, N*C*H$_2$COO), 77.62 (O*C*H$_2$CH), 117.24 (quart, J = 293 Hz, F$_3$*C*COO), 122.12, 126.41, 128.62, 132.47, 135.06, 141.21, 154.99 (Ar-*C*), 162.86 (quart, J = 34.8 Hz, F$_3$C*C*OO), 171.70 (*C*ONH). ESI-MS: calc.: m/z = 857.93 (M+3H)$^{3+}$, found: 858.23.

Preparation of 5,11,17,23-tetrakis-(DO3A-py$^{NO–C}$-acetamidyl) 25,26,27,28-tetrapropoxy-calix[4]arene Gd-complex (3). 5,11,17,23-Tetrakis-(DO3A-py$^{NO–C}$-acetamidyl)-25,26,27,28-tetrapropoxy-calix[4]arene (88.8 mg of the crude compound) was dissolved in water (20 ml) and GdCl$_3$·6H$_2$O (51.4 mg, 138 μmol) was added. The pH was slowly adjusted to 7 using aqueous NaOH and the solution was stirred for 1 d. EDTA (40 mg, 138 μmol) was added

and the pH kept between 5.5 and 7.5. After stirring for another 3 h, the Gd(III)-complex was purified by ultrafiltration (500 Da membrane, solvent: water) and obtained after lyophilisation as a yellow powder (45.0 mg, *ca.* 60% yield). ESI-MS: calc.: $m/z = 1085.42$ (M+3Na)$^{3+}$, found: 1085.25.

Sample preparation

Compound **3** was dissolved in water containing small amounts (0.5%) of ^{17}O-enriched water and *tert*-butanol as internal standard. The gadolinium concentration was determined by bulk magnetic susceptibility (BMS) measurements using acidified water containing a small amount of *tert*-butanol as external standard.[26] All further measurements were performed using this solution (91.7 mM Gd, 22.9 mM **3**) as a stock solution.

^{17}O NMR

These measurements were performed on a Varian Inova-300 spectrometer (40.7 MHz). T_1 relaxation times were measured by the standard inversion recovery pulse sequence. T_2 relaxation times were determined by the Carr-Purcell-Meiboom-Gill spin echo pulse sequence. No frequency lock was used and the samples were not spun. The chemical shifts (in ppm) were corrected for the BMS by using a reference of acidified water having *tert*-butanol as internal standard. To ensure temperature equilibration, the samples were kept in the probe for at least 10 min prior to the measurements.

^1H NMRD

The ^1H NMRD profiles were recorded on a Stelar Smartracer FFC fast-field-cycling relaxometer covering magnetic fields from 2.35×10^{-4} T to 0.25 T, which corresponds to a proton Larmor frequency range of 0.01-10 MHz. The relaxivity at higher fields was recorded using a Bruker WP80 with the Spinmaster Smartracer PC-NMR console at variable field from 20 MHz to 80 MHz. The temperature was controlled by a VTC90 temperature control unit and fixed by a gas flow. The temperature was determined according to previous calibration with a Pt resistance temperature probe. All samples were kept in the probe for at least 10 min to equilibrate the temperature prior to the measurement.

Fittings of NMR data

All fittings were performed using the Micromath Scientist program with the least-square procedure and the commonly used equation set.[19,21] For some of the parameters describing the NMRD profiles, commonly accepted values were used such as for the distance between Gd(III) and a proton of coordinated water (r_{GdH}) 3.1 Å and the distance of the closest approach of an outer sphere water proton to Gd(III) 3.5 Å. The activation energy for the electronic rotational correlation time (E_v) was fixed at 1 kJmol^{-1} and the parameter determining the spin rotation contribution to the electron spin relaxation (δg_L) at 0.021.[19] The diffusion coefficient and its activation energy were fixed to the values of pure water.[27]

DLS

Dynamic light scattering (DLS) was performed on a Zetasizer NanoZs, Malvern, UK instrument. The samples measured prior to filtration through a 0.2 μm syringe filter showed identical spectra to those after filtration.

Acknowledgements

Notes and references

1 É. Tóth and A. E. Merbach, *The Chemistry of Contrast Agents in Medical Magnetic Resonance Imaging*, Wiley, Chichester, UK, 2001.
2 P. Caravan, *Chem. Soc. Rev.*, 2006, **35**, 512.
3 P. Caravan, J. J. Ellison, T. J. McMurry and R. B. Lauffer, *Chem. Rev.*, 1999, **99**, 2293.
4 S. Aime, M. Fasano and E. Terreno, *Chem. Soc. Rev.*, 1998, **27**, 19.
5 S. Aime, S. G. Crich, E. Gianolio, G. Giovenzana, L. Tei and E. Terreno, *Coord. Chem. Rev.*, 2006, **250**, 1562.
6 M. Bottrill, L. Kwok and N. J. Long, *Chem. Soc. Rev.*, 2006, **35**, 557.
7 D. T. Schühle, J. Schatz, S. Laurent, L. Vander Elst, R. N. Muller, M. C. A. Stuart and J. A. Peters, *Chem.–Eur. J.*, 2009, **15**, 3290.
8 L. Mandolini and R. Ungaro, *Calixarenes in Action*, Imperial College Press, London, 2000.
9 J. Vicens, J. Harrowfield and L. Baklouti, *Calixarenes in the Nanoworld*, Springer, Dordrecht, 2007.
10 J. Vicens and V. Böhmer, *Calixarenes, a Versatile Class of Macrocyclic Compounds*, Kluwer, Dordrecht, 1991.
11 M. Polášek, J. Rudovský, P. Hermann, I. Lukeš, L. Vander Elst and R. N. Muller, *Chem. Commun.*, 2004, 2602.
12 M. Polášek, M. Šedinová, J. Kotek, L. Vander Elst, R. N. Muller, P. Hermann and I. Lukeš, *Inorg. Chem.*, 2009, **48**, 455.
13 M. Polášek, J. Kotek, P. Hermann, I. Císařová, K. Binnemans and I. Lukeš, *Inorg. Chem.*, 2009, **48**, 466.
14 M. Polášek, P. Hermann, J. A. Peters, C. F. G. C. Geraldes and I. Lukeš, *Bioconj,. Chem.*, in press.
15 J. Klimentová and P. Vojtíšek, *J. Mol. Struct.*, 2007, **826**, 48.
16 P. Lindner and T. Zemb, *Neutrons, X-rays and Light: Scattering Methods Applied to Soft Condensed Matter*, Elsevier, Amsterdam, 2002.
17 J. P. André, É. Tóth, H. Fischer, A. Seelig, H. R. Mäcke and A. E. Merbach, *Chem.–Eur. J.*, 1999, **5**, 2977.
18 D. H. Powell, O. M. N. Dhubhghaill, D. Pubanz, L. Helm, Y. S. Lebedev, W. Schlaepfer and A. E. Merbach, *J. Am. Chem. Soc.*, 1996, **118**, 9333.
19 N. M. Gaëlle, É. Tóth, K. Eisenwiener, H. R. Mäcke and A. E. Merbach, *JBIC, J. Biol. Inorg. Chem.*, 2002, **7**, 757.
20 H. Kobayashi and M. W. Brechbiel, *Adv. Drug Delivery Rev.*, 2005, **57**, 2271.
21 L. Helm, *Prog. Nucl. Magn. Reson. Spectrosc.*, 2006, **49**, 45.
22 J. B. Livramento, É. Tóth, A. Sour, A. Borel, A. E. Merbach and R. Ruloff, *Angew. Chem.*, 2005, **117**, 1504.
23 L. H. Bryant Jr., A. T. Yordanov, J. J. Linnoila, M. W. Brechbiel and J. A. Frank, *Angew. Chem., Int. Ed.*, 2000, **39**, 1641.
24 S. Aime, A. Barge, M. Botta, A. Casnati, M. Fragai, C. Luchinat and R. Ungaro, *Angew. Chem., Int. Ed.*, 2001, **40**, 4737.
25 S. Dumas, J. S. Troughton, N. J. Cloutier, J. M. Chasse, T. J. McMurry and P. Caravan, *Aust. J. Chem.*, 2008, **61**, 682.
26 D. M. Corsi, C. Platas-Iglesias, H. van Bekkum and J. A. Peters, *Magn. Reson. Chem.*, 2001, **39**, 723.
27 L. Vander Elst, A. Sessoye, S. Laurent and R. N. Muller, *Helv. Chim. Acta*, 2005, **88**, 574.